International Journal of Chemical and Biochemical Sciences
(ISSN 2226-9614)

Journal Home page: www.iscientific.org/Journal.html

Efficient removal of Orange G Dye from Wastewater using an economical PANI@Clay adsorbent and Response Surface methodology

Asmaa Khattari [1], Mohamed Farah[1], Fatima Zahra Addar [1], Jaouad Bensalah [1], Abdelghani Hsini [1, 2], Abdelillah Shaim [1], Mustapha Tahaikt [1], Azzedine Elmidaoui [1]*

[1]*Laboratory of Advanced Materials and Process Engineering (LAMPE), Department of Chemistry, Faculty of Sciences, Ibn Tofaïl University, B.P. 133, 14000 Kenitra, Morocco.*

[2]*National Higher School of Chemistry (NHSC), University Ibn Tofail, BP. 133-14000, Kenitra, Morocco.*

Abstract

This study sought to evaluate the practicality and cost-effectiveness of employing a natural clay coated with polyaniline (PANI) polymer for eliminating cationic dyes, specifically Orange G (OG), from aqueous solutions. Various analytical techniques, including FTIR, XRD, SEM, and EDS, were utilized to scrutinize the characteristics of the resulting adsorbent. Efficiency assessments of OG dye adsorption were conducted under diverse conditions, encompassing adsorbent mass, pH, and initial dye concentration. To optimize efficiency, a customized experimental strategy utilizing Response Surface Methodology (RSM) was implemented, comprising 24 sets of experiments to assess the impact of key variables such as adsorbent dose (A), pH (B) and initial dye concentration (C), as well as their interactions. Statistical analysis underscores the significant importance of the removal model, supported by an exceedingly low probability value ($p < 0.0001$). Specifically, heightened adsorbent quantity and solution pH correlated with increased OG removal rates, while an elevated initial dye concentration resulted in a decreased removal rate. Additionally, the interaction between these variables was deemed insignificantly influential. Experimental findings showcased a peak OG removal efficiency of 96.80%, achieved with an adsorbent mass of 17.36 mg, a pH of 6.88 and an initial dye concentration (IC) of 20.39 mg/L. The equilibrium adsorption capacity of PANI@Clay was determined to be 69.5 mg/g, surpassing the 48.6 mg/g observed in raw clay. This comprehensive approach offers valuable insights into adapting the adsorption process for effectively eliminating cationic dyes using PANI@Clay-coated clay. The adsorption kinetics of OG dye onto the adsorbent were accurately described by a pseudo-second-order equation. Furthermore, experimental results indicated that the Langmuir model exhibited significantly better fitting than the Freundlich model.

Keywords: Adsorption, Orange G dye removal, PANI@Clay, Regeneration, Modelling, RSM.

Full length article **Corresponding Author*, e-mail: mohamed.farah@uit.ac.ma

1. Introduction

Synthetic dyes used in textile production generate effluent that adds significantly to water pollution. Large amounts of colorful effluent containing organic compounds that are tough to handle are emitted as a result of the usage of these dyes. The potential dangers these dyes bring to aquatic ecosystems and human health make it all the more important to find effective treatment solutions for them [1-3]. Among the various possible treatment methods, such as coagulation and flocculation, electrodialysis, chemical precipitation, biological processes, membrane separation, and adsorption, adsorption treatment is favored when it comes to clarifying wastewater, due to its low cost, broad applicability, and minimal environmental impact [4]. It is easy to scale up adsorption for industrial purposes, and it can remove a lot of color even from dilute solutions [5]. Activated carbon is just one form of adsorbent that serves this function, chitosan, zeolites, clay minerals, and the different types of bio-adsorbents [6-11]. However, the utilization of any of these adsorbents comes with its set of limitations, including high costs, challenges in regeneration, and low selectivity. In an effort to address these constraints, researchers are exploring the development of a novel adsorbent material by combining natural clay with cellulose acetate [12]. Capitalizing on the combined adsorptive capabilities of natural clay and the efficiency of cellulose acetate in dye adsorption, it is anticipated that the composite material will exhibit a greater adsorption capacity than either component used independently [13].

Natural clays, renowned for their extensive porosity and large surface area, have demonstrated effectiveness as adsorbent materials in previous studies [14]. Additionally, cellulose acetate for dye adsorption has been extensively studied and is generally recognized as an efficient and environmentally friendly approach [15]. The evaluation focuses on a new composite adsorbent material, resulting from the combination of the PANI polymer with raw clay, in the context of adsorbing the orange dye (OG), a commonly used adsorbent [16]. Orang G (OG) dye with excellent stability and resistance to degradation, will serve as a reference for this investigation. That's why it's harder to get rid of in wastewater treatment plants than other pigments [17]. In order to analyze the adsorption behavior of the composite adsorbent (PANI@Clay), we will use the adsorption isotherm data of Orange G (OG). Various adsorption equations and models, as well as ultraviolet-visible spectroscopy will be employed to examine the adsorption properties of raw clay and PANI@Clay in order to learn more about how adsorption works and how quickly it happens. Despite the prevalence of illite in our raw clay, no computer research has yet investigated OG adsorption on the clay's surface. Since this approach has been employed by a number of writers before, we will use molecular dynamics simulations to assess OG removal from water and to research the ways in which the altered and unaltered clays absorb substances [18]. This study's findings should help inform a strategy for treating textile wastewater that is both effective and sustainable. The Response Surface Methodology (RSM) is a statistical approach aimed at determining the optimal parameters of a process and solving multivariate problems. This method relies on a rigorous experimental design, data collection through experiments, and the use of a multivariate quadratic regression equation to model the functional relationship between factors and response values [19]. Historically, RSM has found broad application in various chemical fields such as water treatment, materials synthesis, waste treatment, air pollution control, among others. Its use helps minimize the number of experiments, optimize processes, and conduct graphical and regression analyses [20-23]. However, it is important to note that most of the previously mentioned applications have been carried out in the context of homogeneous and stable systems. The application of RSM for modeling and optimizing heterogeneous and unstable systems has been rarely reported. The most commonly used experimental designs in RSM include the composite central design (CCD), the Box-Behnken design (BBD), the user-defined design, and the customized model based on historical data [24-25]. In this study, the PANI@Clay composite was employed for the removal of the orange dye (OG). A customized experimental design, based on the Response Surface Methodology (RSM), was implemented to analyze how the adsorbent dose (A), pH (B), and initial dye concentration (C) simultaneously influence the removal rate of OG (Y). The primary objective was to determine the optimal conditions to maximize the desired response. A second-order polynomial mathematical model was used to establish the relationship between these variables, and its validity was confirmed through analysis of variance (ANOVA) to assess its statistical significance.

2. Materials and methods

2.1. Materials

2.1.1. Fabrication of PANI@Clay composite

Only bi-distilled water used to make all of the solutions. and polyaniline (PANI) purchased from Sigma-Aldrich. The natural clay utilized here comes from Morocco, specifically the Khemisset region. By crushing the clay, smaller fractions with diameters less than 56 m were achieved, screening using a typical ASTM sieve, and drying in an oven at 105 °C for 24 hours. The unprocessed Orange G was provided by the University of Ibn Tofail Laboratory of Chemistry. To make the dye solution, 1 gram of OG mixed with 1 liter of bi-distilled water. Additional diluting was carried out until the desired concentrations were attained [22].

2.2. Methods

The procedure begins with purifying the polyaniline ($C_6H_5NH_2$). All other chemical reactants used were of analytical quality and came from Sigma-Aldrich; these were HCl, $Na_2S_2O_8$, acetone, NaOH, and ethanol. The OG stock solution was prepared using distilled water.

2.3. Batch experiments

By dissolving 0.015 g of PANI@Clay in 40 mL of OG at starting values between 20 and 400 mg, we were able to conduct adsorption tests on the PANI@Clay composite until equilibrium was attained. The effects of pH were examined throughout a range of values, from 2 to 12, by using small quantities of concentrated HCl or NaOH solutions to alter the pH. At 298K, the kinetics of the reaction between 20 mg of OG and 0.75 g of adsorbent per liter of solution were studied. The following formulas were used to determine the adsorption capacity Qe (mg/g) and the OG removal (%):

$$R(\%) = \frac{(C_0 - C_e)}{C_0} \times 100 \quad (1)$$

$$Q_e = \frac{(C_0 - C_e)}{m} \times V \quad (2)$$

C_0 (mg/L) and C_e (mg/L) represent the initial and equilibrium concentrations of OG dye; m (g) and V (L) represent the mass of the PANI@Clay composite and the volume of the solution, respectively.

2.4. Response surface methodology

This study employed a tailored historical design methodology to establish the correlation between operational variables and response. The process variables utilized in this experimental design are outlined in Table 1, with two levels chosen for each of the three factors and the response variable. A quadratic polynomial model is used in this study, as presented in equation (3) [26].

$$y = a_0 + \sum_{i=1}^{n} a_i x_i + \sum_{i=1}^{n} a_{ii} x_i^2 + \sum_{i=1}^{n} \sum_{j=i+1}^{n} a_{ij} x_i x_j \quad (3)$$

Here, Y (%) denotes the OG dye removal rate, serving as the response variable. X_i and X_j stand for the chosen independent variables.

While a_0 represents the model constant. The coefficients a_i, a_{ii}, and a_{ij} correspond to the regression coefficients for the

linear, quadratic, and interaction terms, respectively, within the model. The model's efficacy is assessed through ANOVA analysis of its results. Recent studies highlight two primary methods model significance and non-significance as suitable indicators for response prediction, gauging the alignment between the predicted model and experimental outcomes [27-30].

3. Results and discussion

3.1. Characterization of the adsorbent

3.1.1. X-ray diffraction

La Figure 1 displays the X-ray powder diffractograms of PANI@clay, indicating that the PANI@clay fraction is mainly composed of muscovite, with a low content of dolomite and a pronounced presence of calcite. The XRD diffractogram of the raw red clay, as illustrated in Figure 2, reveals distinct features. Quartz contributes to reflections at 2θ = 26.74° and 20.97°, while calcite ($CaCO_3$) is responsible for reflections at 2Θ = 29.22° and 31.2° [31]. Kaolinite-typical peaks, such as those at 12.45 and 25.04, are evident in addition to the d_{001}= 7.10 and its harmonic d_{002}= 3.55 peaks. Both illite and chlorite clay fractions manifest the 8.83 reflection with a base distance of d_{001}=10.00. The results suggest a singular type of charge-balancing cations, likely connected to potassium (K), occupying the interfoliar gaps of the illite in this clay. The broad illite peak indicates the phyllosilicate's relatively low crystallinity compared to the mentioned accessory minerals. Prior investigations demonstrated the absence of a smectite phase in the PANI@Clay diffractogram due to the negligible displacement of characteristic reflections [32-33].

3.1.2. FT-IR Spectroscopy

In order to better define the PANI@Clay composite. The Fourier transform of infrared spectra is gaining popularity. Combining the FT-IR spectra in the (Figure 2). FT-IR enables a quantitative exploration of bonding processes. The experiment aimed to evaluate the surface functional groups and interactions of the clay. The FT-IR spectra of the clay, depicted in Figure 2 both before and after the adsorption of OG and PANI@Clay. In Figure 2, the clay spectra show the presence of a carbonate band at 1424 and 693.4 cm^{-1}. Even post-adsorption, the red clay spectrum retains two small bands at 797 and 778 cm^{-1}, both associated with quartz. The band at 3624 cm^{-1} corresponds to the elongation vibrations of hydroxyl (OH) groups bound to Al^{3+} ions, and the band at 918 cm^{-1} is due to deformation. The Si-O bond's elongation vibrations contribute to the bands at 1021 and 1118 cm^{-1}, while the deformation vibrations account for the bands at 532 and 466 cm^{-1} [31]. The presence of kaolinite is indicated by the band at 3700 cm^{-1} [33]. XRD examination (Figure 2) confirms the existence of calcite, quartz, and kaolinite, aligning with the FT-IR findings. Characteristics of the PANI polymer are evident in the bands at 1732, 1368, and 1232 cm^{-1}, as depicted in Figure 2. Notably, the interactions between the raw clay and PANI polymer contribute to the broad frequency range observed at 1732 cm^{-1} [34]. Following OG dye adsorption, two new bands emerge at 1587 cm^{-1} and 1365cm^{-1} (Figure 2), associated with -C- -C- and C- -N- stretching. These bands provide insights into the extent of OG dye absorption by PANI@Clay.

3.1.3. SEM/EDX

The elemental chemical composition of the clay was subjectively estimated with the use of analytical microscope (SEM) and an energy dispersion X-ray spectrometer (EDS) (Figure 3). The raw clay and the PANI@Clay are shown in Figure 3. Figure 3 (a) shows a micrograph with a wide variety of particle sizes and pore diameters, while Figure 3 (b) shows a micrograph with no porosity after modification. Al, Fe, Mg, Si, O, and other elements make up the phyllosilicates, whereas impurities like Na and K may be seen in the EDS spectrum shown in Figure 3 (a). Figure 3 (b) shows that carbon was produced as a result of the reaction between PANI and the unprocessed clay. Table 1 shows that the raw clay has a larger percentage of silicon and oxygen and a lower amount of aluminum. This outcome may have been attained because of compensating factors that are not clay. In addition, the significant amount of carbon present and the lack of carbonate impurity revealed by XRD technique provide further evidence that PANI has modified the raw clay.

3.2. RSM modeling

To streamline the analysis, the experimental data were input into Design Expert software (version 13), effectively characterizing the efficacy of the OG removal adsorption process. Employing a customized design (CD) generated a design matrix, detailed in Table 2. Through the evaluation of these results, a conclusive empirical model was formulated. This model delineates the interactions among different variables in the adsorption process (adsorbent dose (A), pH (B), IC (C)) and the resulting response (OG removal rate (Y)). The mathematical expression capturing this relationship is encapsulated in equation (4):

$$Y = 41.30 + 30.70 * A - 4.15 * B - 31.75 * C - 20.8 * A^2 - 43.62 * B^2 + 12.52 * C^2 \quad (4)$$

The efficacy of the constructed model was evaluated concerning its fit and significance via ANOVA. The results, with a specific focus on OG removal as the response variable, are delineated in Table 3. The regression equations indicated that variables A and C^2 positively influenced the response, whereas variables B, C, A^2 and B^2 had negative effects. Interactions AB, AC, and BC displayed zero effects, indicating a minimal impact from these interactions.

3.2.1. Analysis of variance

Analyzing the ANOVA results in Table 3 for the OG dye, the most influential effects can be ranked in the following order:

$$C > A > B^2 > A^2 > C^2 > B$$

For the OG removal model, interactions AB, AC, and BC were found to be non-significant. The (Y) model underwent evaluation through the F-value (68.07) and the p-value (less than 0.0001).

The latter indicates high statistical significance, with a mere 0.01% chance of an error occurring by chance. Typically, a model is deemed significant when the p-value is below 0.0500, and in this instance, the obtained results affirm the model's significance. Furthermore, the R^2 value of the

model stands at 0.96, indicating an excellent concordance between the modeled outcomes and experimental observations. Consequently, the regression model proves capable of predicting and simulating the OG dye adsorption process as a function of the independent variables. Figure 4 illustrates the comparison between experimentally obtained values and those predicted by equation (3). With a coefficient of determination (R^2) at 0.96, the even distribution of predicted values in close proximity to actual values showcases a robust fit. This high R^2 value signifies a strong correlation between the model's predictions and the actual outcomes, affirming the reliability and credibility of the model equations. Fundamentally, these findings emphasize the resilience of the model and its capacity to precisely anticipate response values under conditions resembling those of the experiment.

3.2.2. 3D response surfaces

Figure 5 depicts response surface plots illustrating the interaction effects among three parameters: adsorbent dose (A), pH (B), and initial dye concentration (C) on the response (OG). These 3D response surfaces offer a precise visualization of the collective influence of these variables on the response. The information presented in Figure 5 clearly demonstrates the substantial impact of the examined parameters—adsorbent dose (A), pH (B), and initial concentration (C)—on the efficiency of OG removal. Generally, an upward trend in these parameters corresponds to an increase in the elimination rate, except for initial concentration (C), where a higher value results in a decrease in the elimination rate. Notably, pH has a more pronounced effect at 6. Moreover, the interactions among these parameters are deemed insignificant, as confirmed by the regression equations. It is crucial to highlight the statistical significance of these findings. Nonetheless, from an experimental perspective, the adsorbent dose stands out as a pivotal factor in dye removal from wastewater.

3.2.3. Optimization

The results of the Response Surface Methodology (RSM) optimization, with the objective of maximizing the removal rate of OG under optimal conditions and across all independent variables, are presented in Figure 6 & Table 4. The adsorptive dye removal process underwent optimization through the utilization of Design Expert software. The primary aim was to enhance OG removal by examining independent variables within the experimental range. The optimal solution was chosen based on the highest desirability or its proximity to unity, usually falling within the red zone denoting maximum removal efficiency. Under the optimal conditions of adsorbent mass at 17.36 mg, pH at 6.88, and initial concentration at 20.39 mg/L, OG removal efficiency reached 96.80%. It's important to highlight that this optimization was conducted utilizing the adsorption method.

3.3. Adsorption study

3.3.1. Effects of adsorbent dose and pH

It is well-known that adsorbent dose has a significant effect on the overall cost of the adsorption process. Here, we investigated the effects of changing the PANI@Clay concentration from 0.125 to 1 $g.L^{-1}$ on OG adsorption. The percentage of OG removed rose dramatically with increasing PANI@Clay dose, as shown by the experimental data in Figure 7 (a). This pattern is clearly explained by the fact that as the mass of PANI@Clay rises, as does the frequency of interactions between adsorbents. Studies of adsorption capacity revealed that concentrations of OG dye as high as 0.75 g/L. Due to the fixed OG dye concentration in the solution phase, the adsorption performance was relatively unaffected by an increase in the PANI@Clay dose beyond 0.75 g/L. Therefore, 0.75 g/L adsorbent was selected for further study. Water solubility, surface functional groups, and the degree to which metal ions are ionized are all affected by the material's pH. It is widely known that acidic and alkaline prepared material surface locations are preferentially adsorbent for OG dye.

3.3.2. Adsorption kinetics and isotherm

To identify the potential adsorption phase between OG and PANI@Clay adsorbent surface sites, a kinetic analysis is thought to be a vital feature in adsorption research. Figure 8 (a) shows that within the first 5 minutes, OG was rapidly adsorbed over the PANI@Clay composite surface sites, then gradually slows down, and finally achieves equilibrium point at 60 min. Several kinetic models were then used to the gathered experimental data for a more thorough analysis. Table 4 lists the regression parameters for the faux 1^{st} order model, the pseudo 2^{nd} order model, and the intra particle diffusion model. The adsorption of OG ions over the PANI@Clay surface sites followed a pseudo 2nd order model, as indicated by the regression coefficients (R^2). The computed adsorbed amounts (Qe) also closely matched the obtained experimental values, indicating a better fit. The results further suggest that OG chemisorption over PANI@Clay composite might be the rate limiting step. Furthermore, In Figure 8 (b), we see the intra-particle diffusion model fitting the adsorption kinetic data. Multilinear profiles of intraparticle diffusion plots clearly show the three stages of OG species transport from the liquid phase to the surface sites of solid materials. In the first phase, OG moves from the water to the PANI@Clay composite interface. At this point, a greater mass flow rate has resulted in a greater amount of OG being transferred from the liquid to the adsorbent phase. Second slower phase highlights the saturation of PANI@Clay surface sites and, the internal diffusion resistance increases, Moreover, pore diffusion mostly regulates the slower second step's pace [35]. The third step is attributed to ultimate adsorption equilibrium due to eventual saturation of adsorbent surfaces sites. Pseudo-first order diffusion rate constants are denoted by k_1 (min^{-1}), pseudo-second order diffusion rate constants by k_2 ($mg.g^{-1}.min^{-1}$), and intraparticle diffusion rate constants by kint ($mg.g^{-1}.min^{-1/2}$). Constant C (mg/g) is proportional to the depth of the boundary layer. Adsorbed quantities are denoted by Qe (mg/g) and Qt (mg/g) at equilibrium and time t (min), respectively.

Table 1: Independent variables, their levels and symbols for CD.

Factor	Name	Units	Minimum	Maximum
A	Adsorbent dose	Mg	2,5	20
B	pH		2	12
C	IC	mg/L	20	400

Table 2: Design Experimental Data.

Run	Factor1 A: Adsorbent Dose (mg)	Factor2 B: pH	Factor3 C: IC (mg/L)	Response: OG Removal (%)
1	2.5	6	20	26.02
2	5.0	6	20	63.16
3	7.5	6	20	68.57
4	10.0	6	20	76.69
5	12.5	6	20	86.77
6	15.0	6	20	92.41
7	17.5	6	20	96.02
8	20.0	6	20	96.77
9	20.0	2	20	50.918
10	20.0	4	20	88.771
11	20.0	6	20	92.867
12	20.0	8	20	87.994
13	20.0	10	20	70.056
14	20.0	12	20	52.895
15	20.0	6	20	93.85
16	20.0	6	50	95.54
17	20.0	6	75	80.28
18	20.0	6	100	70.62
19	20.0	6	150	61.77
20	20.0	6	175	54.88
21	20.0	6	200	50.71
22	20.0	6	300	38.58
23	20.0	6	350	34.1
24	20.0	6	400	30.9

Table 3: ANOVA for the quadratic model of the response surface in OG dye removal.

Source	Sum of Squares	Df	Mean Square	F-value	p-value	
Model	11372.95	6	1895.49	68.07	< 0.0001	Significant
A-Adsorbent dose	4721.36	1	4721.36	169.55	< 0.0001	
B-Ph	49.17	1	49.17	1.77	0.2014	
C-IC	5475.07	1	5475.07	196.62	< 0.0001	
AB	0	0				
AC	0	0				
BC	0	0				
A^2	711.0	1	711.00	25.53	< 0.0001	
B^2	2541.63	1	2541.63	91.28	< 0.0001	
C^2	286.93	1	286.93	10.3	0.0051	
Residual	473.38	17	27.85			
Lack of Fit	465.13	15	31.01	7.52	0.1234	not significant
Pure Error	8.24	2	4.12			
Cor Total	11846.33	23				

Table 4: Parameters for the kinetic model of OG adsorption onto PANI@Clay.

	$Q_{e.exp}$ (mg/g)	Pseudo-1st order $Q_t = Q_e(1 - e^{-k_1 t})$			Pseudo-2nd order $Q_t = \frac{Q_e^2 k_2 t}{1 + Q_e k_2 t}$		
		k_1(min^{-1})	$Q_{e.1}$(mg/g)	R^2	k_2($g.mg^{-1}\cdot min^{-1}$)	$Q_{e.2}$(mg/g)	R^2
PANI@ clay	38.40	0.1114	36.14	0.942	0.00456	39.50	0.985
	Weber–Morris model $Q_t = k_{int} t^{1/2} + C$						
	Initial linear portion			Second linear portion			Third linear portion		
	$k_{int.1}$	C_1	R^2	$k_{int.2}$	C_2	R^2	$k_{int.3}$	C_3	R^2
PANI@ clay	3.106	15.02	0.9741	1.463	25.63	0.9028	0.415	33.51	0.6961

Table 5: The adsorption of OG ions onto PANI@Clay composite is described by Langmuir and Freundlich isotherm expressions, together with the relevant parameters.

Adsorbent	Q_{exp} (mg/g)	Langmuir $Q_e = \frac{Q_{max} K_L C_e}{1 + K_L C_e}$			Freundlich $Q_e = K_F C_e^{1/n}$		
		Q_{max} (mg/g)	K_L ($L\cdot mg^{-1}$)	R^2	n_F	K_F ($mg\cdot g^{-1}$)	R^2
PANI@Clay	247.18	239.30	0.0766	0.9198	4.018	62.91	0.9779

Notation: Qmax (mg/g) is the maximum adsorption capacity, and Ce (mg/L) is the equilibrium intensity [36].

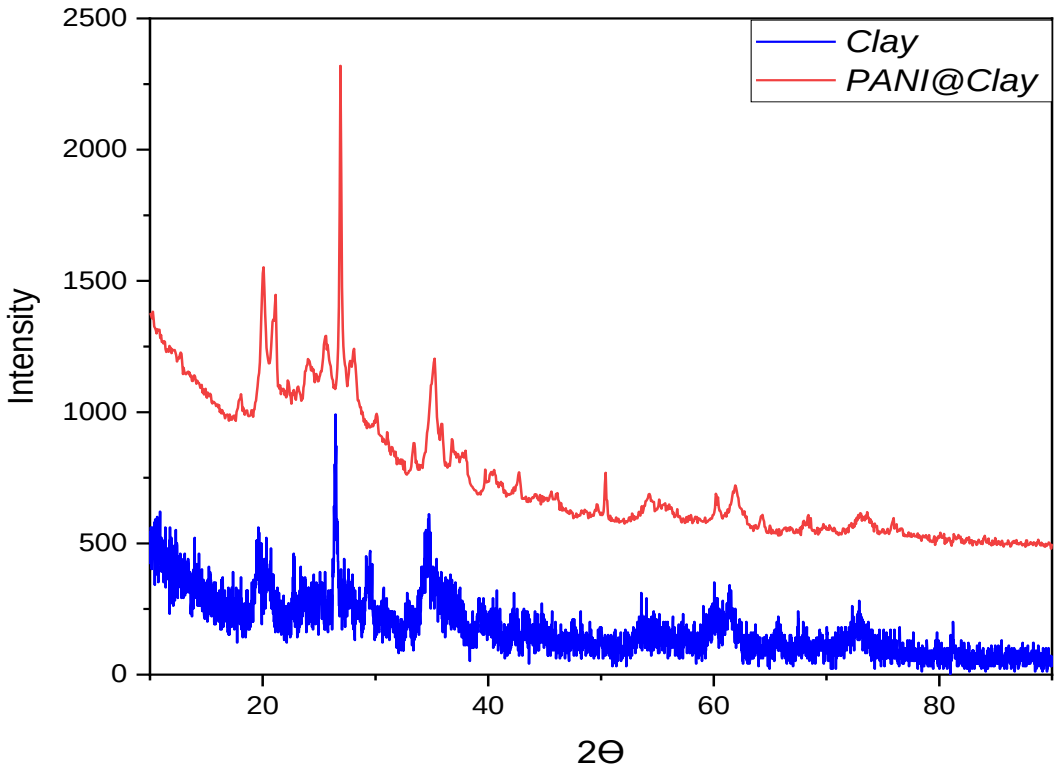

Figure 1: X-ray diffraction spectra of the PANI@Clay composite**.**

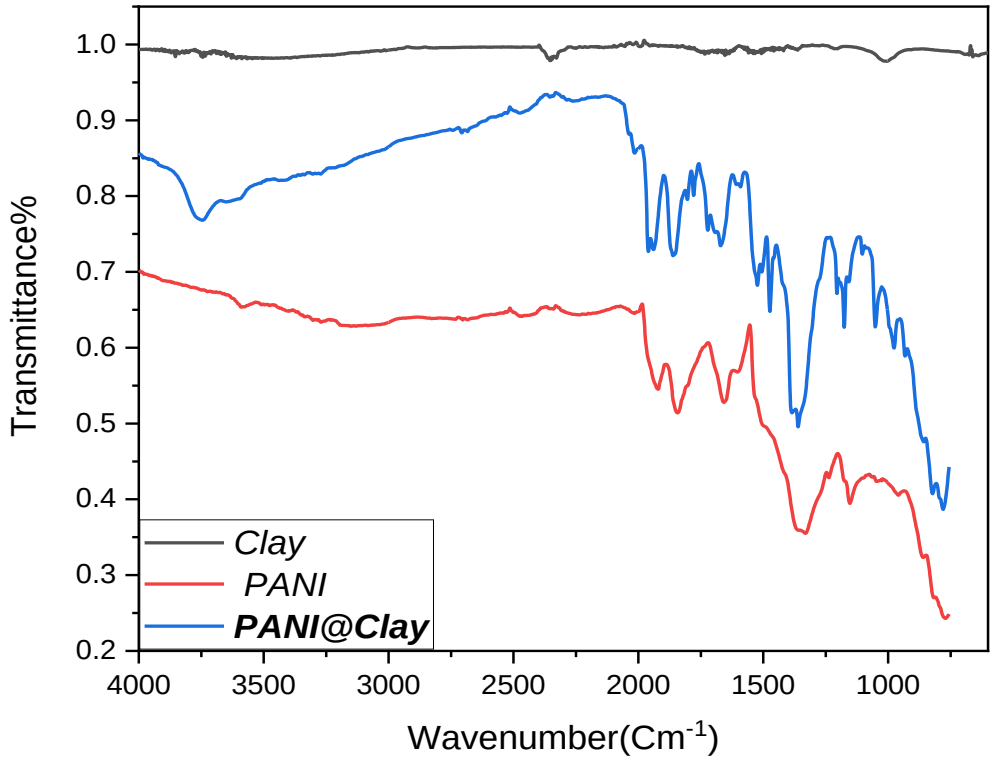

Figure 2. IR spectrum from Clay, PANI and PANI@Clay composite.

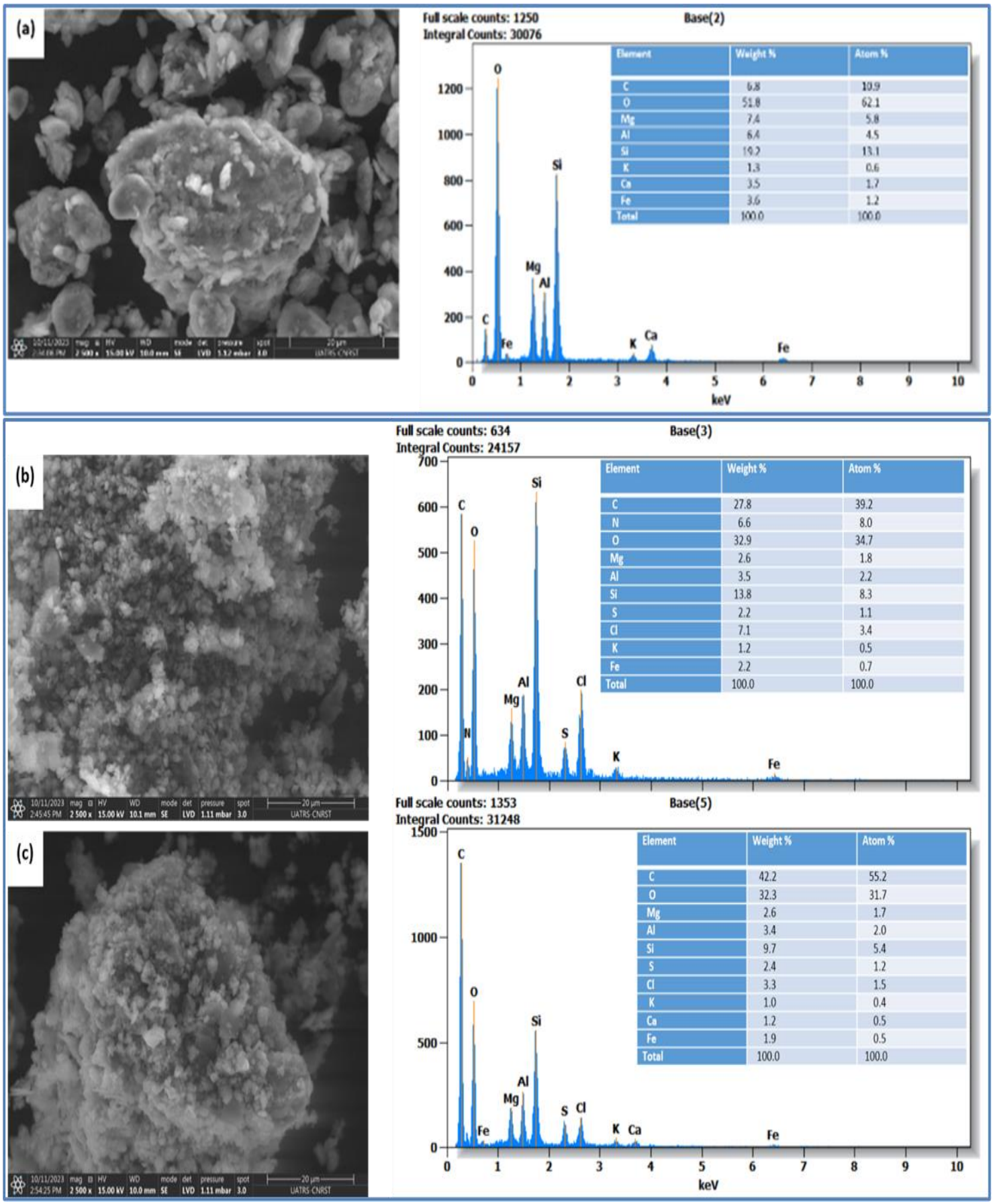

Figure 3: SEM images and respective EDS spectra of the PANI@Clay composite.

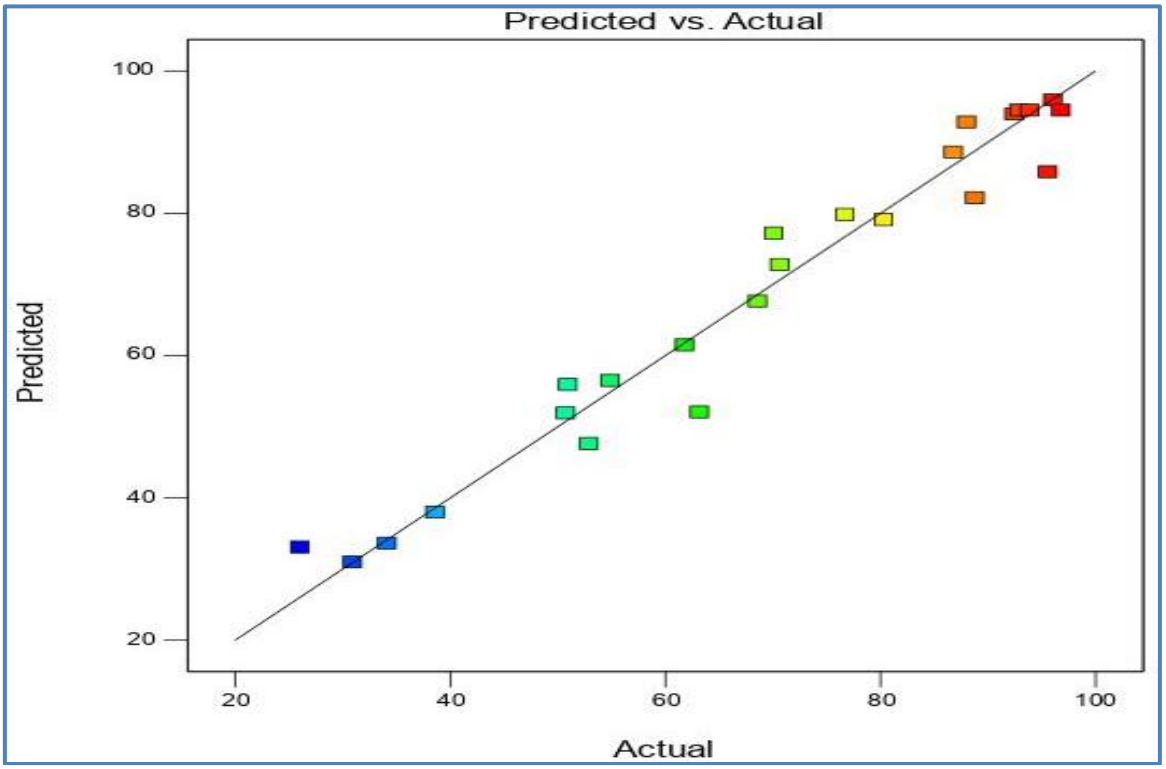

Figure 4: compares the experimental values of OG removal to the predicted data.

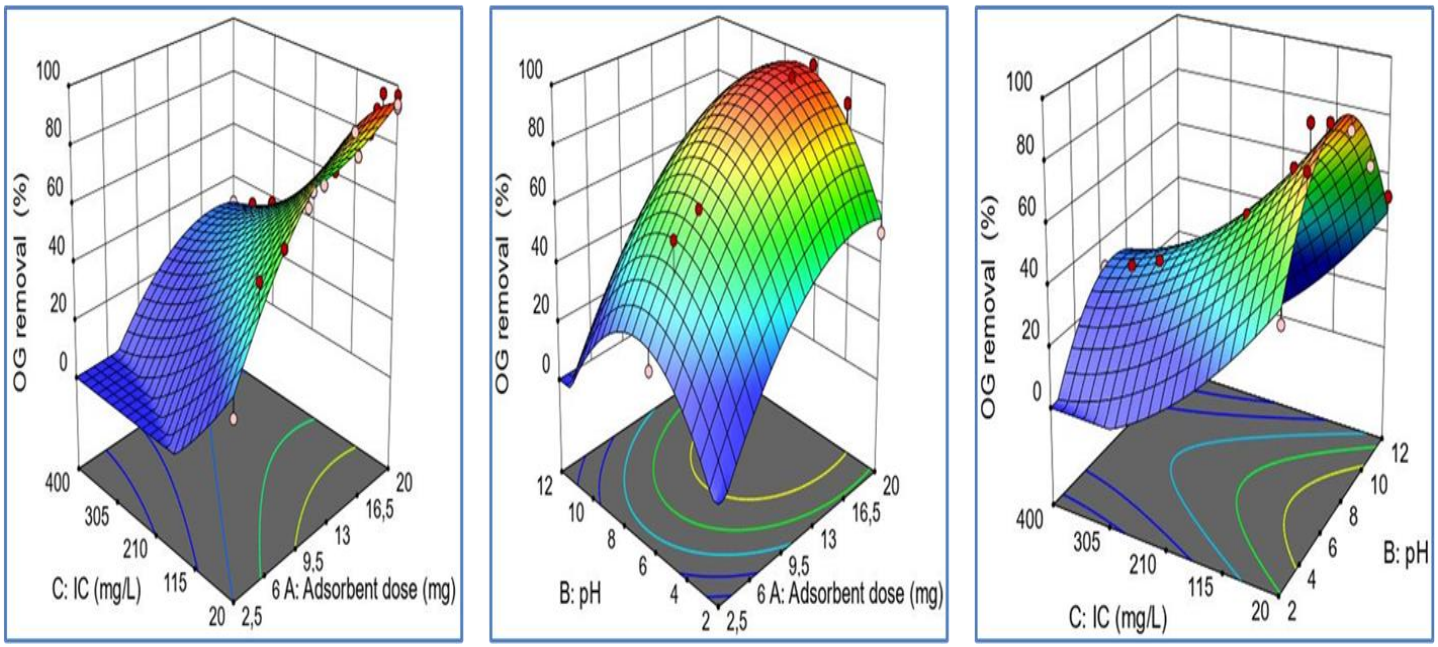

Figure 5: 3D response surfaces illustrating the impact of the interaction among the three parameters (adsorbent dose (A), pH (B), IC (C)) on OG.

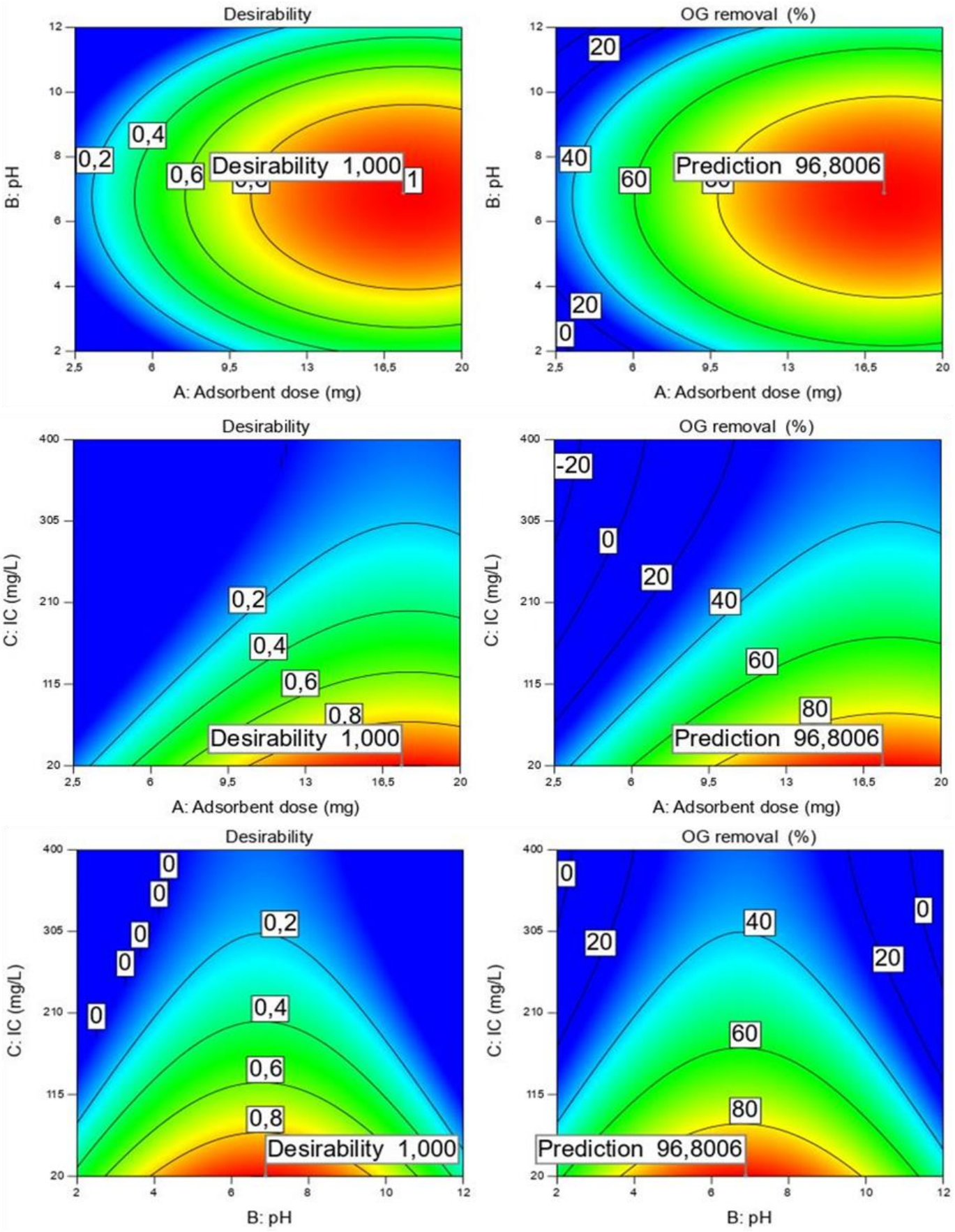

Figure 6: The ideal conditions to maximize the OG removal rate considering the interaction among the three parameters.

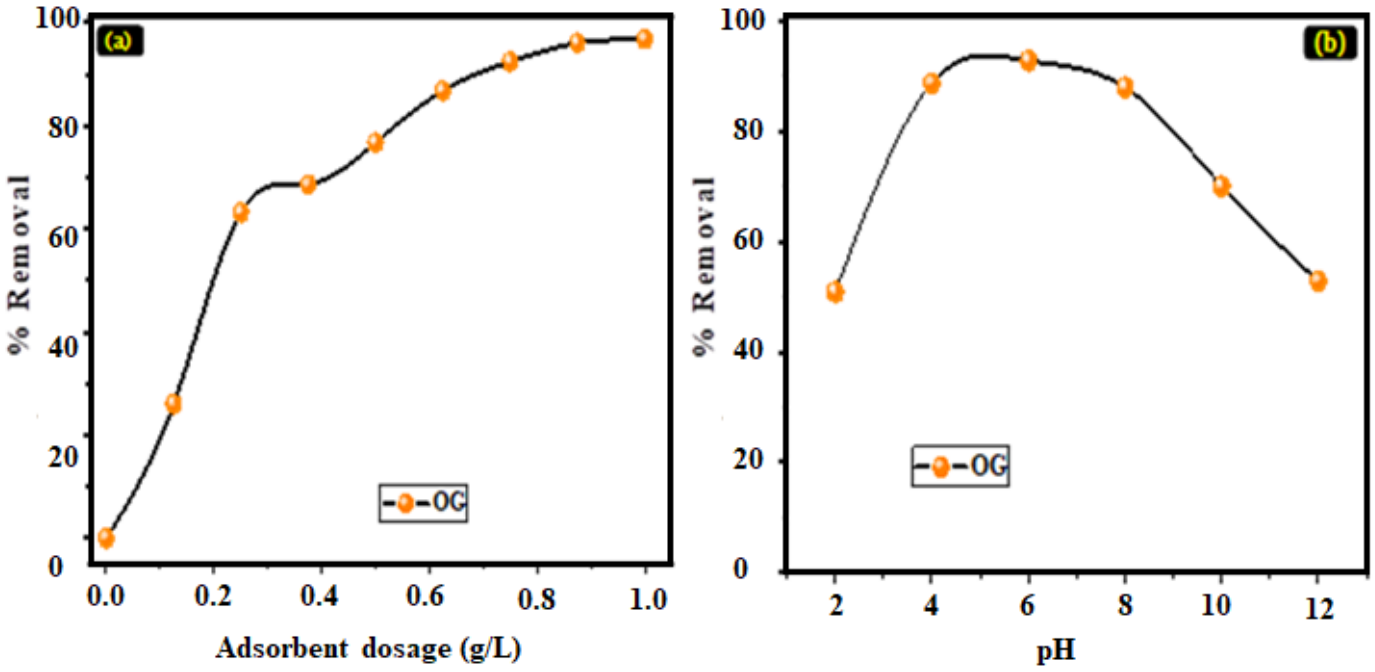

Figure 7: (a) Adsorption efficiency of OG dye using PANI@Clay composite as a function of pH (C_0=20 mg/L, t =60 min, adsorbent dose = 0.75 g/L and T =298K); **(b)** Effect of pH on adsorption efficiency of OG dye.

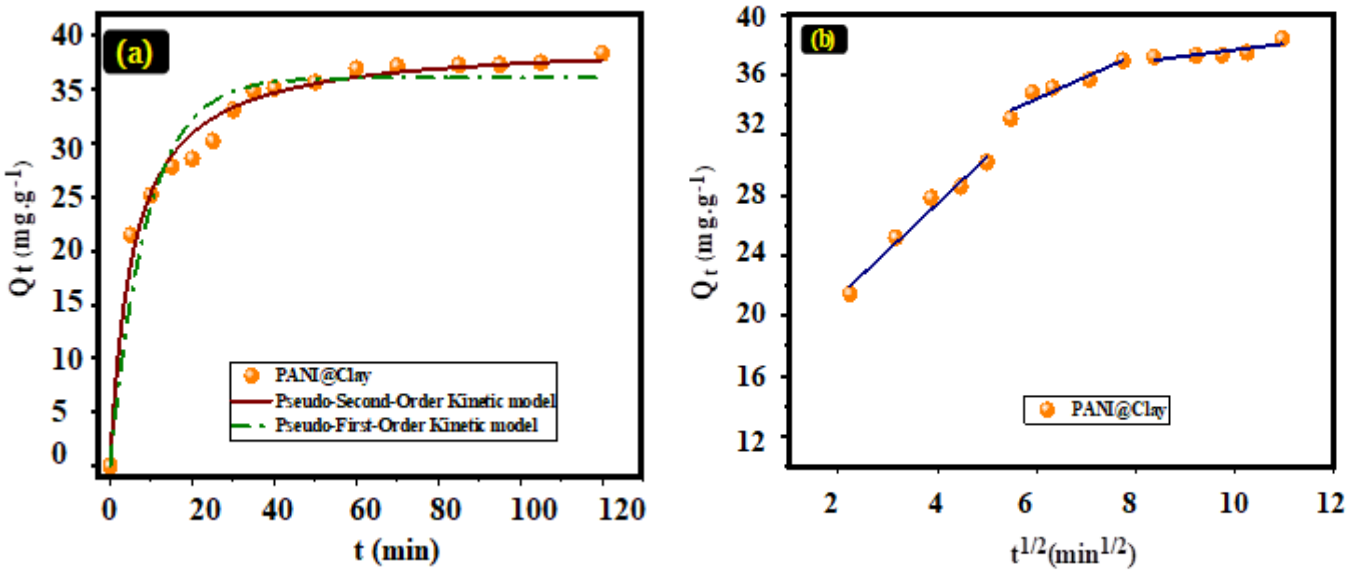

Figure 8: Adsorption of OG by a *PANI@Clay* composite (C_0=20 mg.): pseudo-first order (**a**), pseudo-second order (**a**), and Weber-Morris intra particle diffusion linear (**b**).0.75 g of adsorbent per $L^{-1}.L^{-1}$, T = 298K, pH = 6).

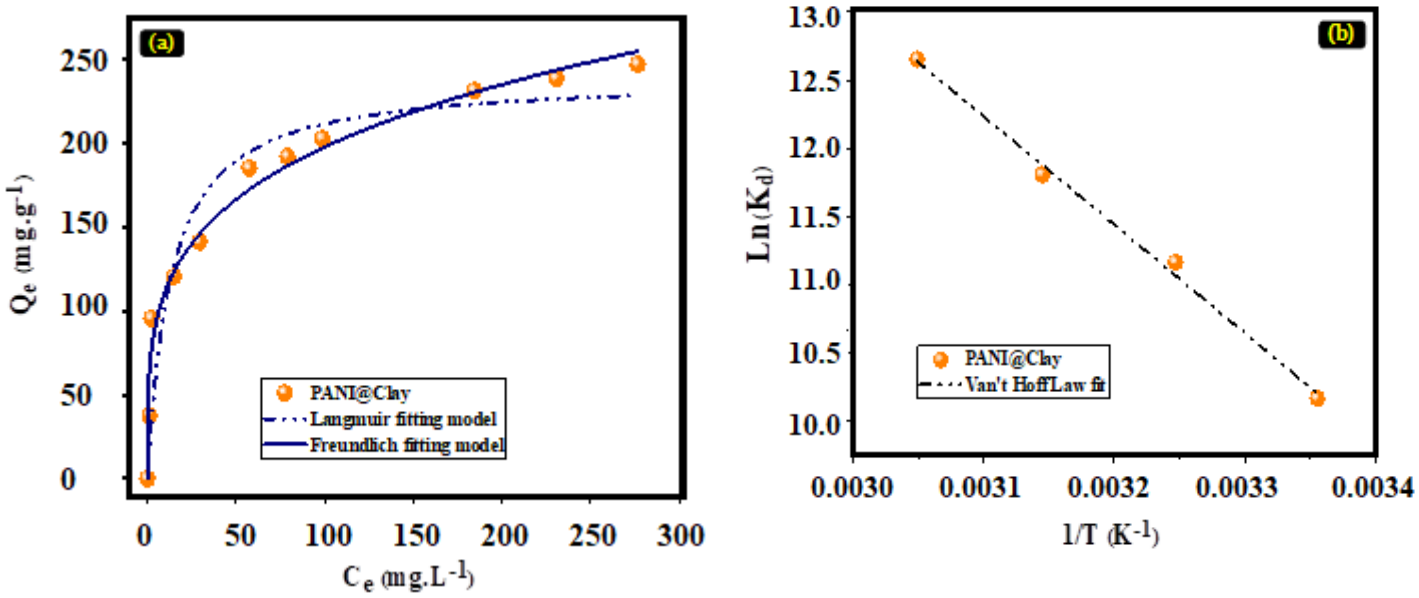

Figure 9: (a) Thermodynamic parameters determined using a non-linear Langmuir and Freundlich isotherm for OG adsorption on the *PANI@Clay* composite.

Prediction of OG removal from bulk liquid to material surface sites relies heavily on an examination of adsorption isotherms. Figure 8 (a) displays the fitted Langmuir and Freundlich isotherms for OG adsorption onto the PANI@Clay composite surface. Table 5 lists the determined values for each parameter. When comparing Freundlich and Langmuir regression coefficient values, it is obvious that the Freundlich model provides a better explanation for the OG ions adsorption data on the PANI@Clay composite. It also suggested that, because of its regular shape, the multilayer OG adsorption phase will be more effective than PANI@Clay surface. The experimental adsorption capacity for PANI@Clay adsorbent towards OG dye is 247.20 mg/g.

4. Conclusions

The results of this investigation show that PANI@Clay is a good adsorbent for OG removal in water. With a maximum equilibrium adsorption capacity that is much greater than that of raw clay, this modified clay shows promise as a sustainable and cost-effective solution for dye and other hazardous material removal from wastewater. The optimal conditions, determined by the RSM method to maximize the removal efficiency of the OG dye (96.80%), are as follows: initial concentration (20.39 mg/L), adsorbent mass (17.36) and pH (6.88). The adsorption process of the OG dye on PANI@Clay was scrutinized using pseudo-second-order kinetics. The isotherm modeling demonstrated an excellent agreement with the Langmuir isotherm. These findings show that PANI@Clay could be employed it is a cost-effective and efficient adsorbent for removing dyes and other hazardous chemicals from water, making it useful in wastewater treatment and environmental remediation. PANI@Clay scalability and practicality for real-world applications require more research.

Acknowledgments

The University Center for Analysis, Technology and Incubation Transfer Expertise (CUAE2TI), under the Ibn Tofaïl University of Kenitra

Declaration of interests

Conflict of interest

The authors declare that they have no known competing financial interests or personal relationships that could have appeared to influence the work reported in this paper.

References

[1] K. Naseem, Z. H. Farooqi, R. Begum, M. Z. Ur Rehman, M. Ghufran, W. Wu, J. Najeeb, A. Irfan. (2020). Synthesis and characterization of poly(N-isopropylmethacrylamide-acrylic acid) smart polymer microgels for adsorptive extraction of copper (II) and cobalt (II) from aqueous medium: kinetic and thermodynamic aspects. Environmental science and Pollution Research. 27: 28169–28182.

[2] A. Nobakht, D. Jafari, M. Esfandyari. (2023). New insights on the adsorption of phenol red dyes from synthetic wastewater using activated carbon/Fe2(MoO4)3. Environmental Monitoring and Assessment. 195 (5): 574.

[3] K. K. Zadeh, D. Jafari. (2023). Activated carbon/alginate/Fe3O4 magnetic nanocomposite as a superior functional material for removal of lead from aqueous media. Biomass Conversion and Biorefinery. 1-19.

[4] M. Zahed, D. Jafari, M. Esfandyari. (2020). Adsorption of formaldehyde from aqueous solution using activated carbon prepared from Hibiscus rosa-sinensis. International Journal of Environmental Analytical Chemistry. 102 (13): 2979-3001.

[5] E. Aboli, D. Jafari, H. Esmaeili. (2020). Heavy metal ions (lead, cobalt, and nickel) biosorption from aqueous solution onto activated carbon prepared from Citrus limetta leaves. Carbon letters. 30: 683-698.

[6] K. Naseem, R. Huma, A. Shahbaz, J. Jamal, M. Z. Ur Rehman, A. Sharif, E. Ahmed, R. Begum, A. Irfan, A. G. Al-Sehemi, Z. H. Farooqi. (2018). Extraction of Heavy Metals from Aqueous Medium by Husk Biomass: Adsorption Isotherm, Kinetic and Thermodynamic study. Zeitschrift für Physikalische Chemie. 233 (2): 201-223.

[7] K. Naseem, Z. H. Farooqi, R. Begum, M. Z. Ur Rehman, A. Shahbaz, U. Farooq, M. Ali, H. M. A. Ur Rahman, A. Irfan, A. G. Al-Sehemi. (2019). Removal of Cadmium (II) from Aqueous Medium Using Vigna radiata Leave Biomass: Equilibrium Isotherms, Kinetics and Thermodynamics. Zeitschrift für Physikalische Chemie. 233 (5): 669-690.

[8] K. Naseem, R. Begum, W. Wu, M. Usman, A. Irfan, A. G. Al-Sehemi, Z. H. Farooqi. (2019). Adsorptive removal of heavy metal ions using polystyrene-poly (N-isopropylmethacrylamide-acrylic acid) core/shell gel particles: Adsorption isotherms and kinetic study. Journal of Molecular Liquids. 277: 522-531.

[9] M. Allaoui, M. Berradi, H. Taouil, H. Es-sahbany, L. Kadiri, A. Ouass, J. Bensalah, S. Ibn Ahmed. (2019). Adsorption of Heavy Metals (nickel) by the Shell Powder of the Coast of Mehdia-Kenitra (Morocco). Analytical & Bioanalytical Electrochemistry. 11 (11): 1547-1558.

[10] J. Bensalah, A. Habsaoui, B. Abbou, L. Kadiri, I. Lebkiri, A. Lebkiri, E. H. Rifi. (2019). Adsorption of the anionic dye methyl orange on used artificial zeolites: kinetic study and modeling of experimental data. Mediterranean Journal of Chemistry. 9 (4): 311-316.

[11] M. Allaoui, M. Berradi, J. Bensalah, H. Es-sahbany, O. Dagdag, S. Ibn Ahmed. (2021). Study of the adsorption of nickel ions on the sea shells of Mehdia: Kinetic and thermodynamic study and mathematical modelling of experimental data. Materials Today: Proceedings. 45: 7494-7500.

[12] J. Bensalah, A. Habsaoui, O. Dagdag, A. Lebkiri, I. Ismi, E. H. Rifi, I. Warad, A. Zarrouk. (2021). Adsorption of a cationic dye (Safranin) by artificial cationic resins Amberlite®IRC-50: Equilibrium, kinetic and thermodynamic study. Chemical Data Collections. 35: 100756.

[13] A. El Amri, J. Bensalah, A. Idrissi, K. Lamya, A. Ouass, S. Bouzakraoui, A. Zarrouk, A. Lebkiri. (2022). Adsorption of a cationic dye (Methylene bleu) by Typha Latifolia: Equilibrium, kinetic, thermodynamic and DFT calculations, Chemical Data Collections. 38: 100834.

[14] A. El Amri, J. Bensalah, L. Kadiri, Y. Essaadaoui, I. Lebkiri, A. Zarrouk, E. H. Rifi, A. Lebkiri. (2022). Investigation of the cellulose reed plant as a potential adsorbent to remove Pb (II): Equilibrium isotherms and thermodynamic studies, Desalination and Water Treatment. 137-151.

[15] A. El Amri, A. Ouass, J. Bensalah, Z. Wardighi, F. Z. Bouhassane, A. Zarrouk, A. Habsaoui, E. H. Rifi, A. Lebkiri. (2023). Extraction and characterization of cellulosic nanocrystals from stems of the reed plant large-leaved cattail (Typha latifolia). Materials Today: Proceedings. 72: 3609-3616.

[16] M. Elabboudi, J. Bensalah, A. El Amri, N. E. Azzouzi, B. Srhir, A. Zarrouk. (2023). Adsorption performance and mechanism of anionic MO dye by the adsorbent polymeric Amberlite®IRA-410 resin from environment wastewater: Equilibrium kinetic and thermodynamic studies. Journal of Molecular Structure. 1277: 134789.

[17] Z. Wardighi, J. Bensalah, A. Zarrouk, E. H. Rifi, A. Lebkiri. (2023). Investigation Adsorption and mechanism of the cationic methylene blue by the polymeric Rubia tinctorum seeds from environment wastewater: Kinetic equilibrium and thermodynamic studies. Desalination and Water Treatment. 300.

[18] J. Bensalah, G. Doumane, O. Iraqi, A. A. Elhenawy, H. Ouaddari, M. K. Okla, H. A. Nafdi, Y. A. Younous, M. Bourhia, A. Habsaoui. (2023). Optimization of an experimental study of cationic Pb metal adsorption by resin polymer. Scientific Reports. 13 (1): 20060.

[19] G. E. P. Box, K. B. Wilson. (1992). On the experimental attainment of optimum conditions. In Breakthroughs in statistics: methodology and distribution (pp. 270-310). New York, NY: Springer New York.

[20] R. Davarnejad, S. Nasiri. (2017). Slaughterhouse wastewater treatment using an advanced oxidation process: Optimization study. Environmental Pollution. 223: 1-10.

[21] G. Yuan, J. Xu, L. Xin, J. Zhu, L. Nie. (2016). Experiment research on mix design and early mechanical performance of alkali-activated slag using response surface methodology (RSM). Ceramics International. 42 (10): 11666-11673.

[22] M. R. Sabour, A. Amiri. (2017). Comparative study of ANN and RSM for simultaneous optimization of multiple targets in Fenton treatment of landfill leachate. Waste management. 65: 54-62.

[23] I. Dahlan, Z. Ahmad, M. Fadly, K. T. Lee, A. H. Kamaruddin, A. R. Mohamed. (2010). Parameters optimization of rice husk ash (RHA)/CaO/CeO2 sorbent for predicting SO2/NO sorption capacity using response surface and neural network models. Journal of hazardous materials. 178 (1-3): 249-257.

[24] S. Benalla, F. Z. Addar, M. Tahaikt, A. Elmidaoui, M. Taky. (2022). Heavy metals removal by ion-exchange resin: experimentation and optimization by custom designs. Desalination and water treatment. 262: 347-358.

[25] M. Zait, F. Z. Addar, N. Elfilali, M. Tahaikt, A. Elmidaoui, M. Taky. (2022). Analysis and optimization of operating conditions on

ultrafiltration of landfill leachate using a response surface methodological approach. Desalination and water treatment. 257: 64-75.

[26] O. Doughmi, M. Farah, F. Z. Addar, A. Hsini, M. Tahaikt, A. Shaim. (2023). Use of oak acorns adsorbent and response surface methodology for removal of crystal violet from aqueous solution. International Journal of Environmental Analytical Chemistry. 1-19.

[27] M. Bahrami, M. J. Amiri, F. Bagheri. (2020). Optimization of Crystal Violet Adsorption by Chemically Modified Potato Starch Using Response Surface Methodology. Pollution. 6 (1): 159-170.

[28] J. Marniemi, M. G. Parkki. (1975). Radiochemical assay of glutathione S-epoxide transferase and its enhancement by phenobarbital in rat liver in vivo. Biochemical Pharmacology. 24: 1569–1572.

[29] F. Z. Addar, S. Qaid, H. Zeggar, H. El Hajji, M. Tahaikt, A. Elmidaoui, M. Taky. (2023). Ultrafiltration of Moroccan Valencia orange juice: juice quality, optimization by custom designs and membrane fouling. Sustainability, Agriculture, Food and Environmental Research. 11.

[30] F. Z. Addar, S. El-Ghzizel, M. Tahaikt, M. Belfaquir, M. Taky, A. Elmidaoui. (2021). Fluoride removal by nanofiltration experimentation, modelling and prediction based on the surface response method. Desalination and water treatment. 240: 75-88.

[31] J. Bensalah, A. Habsaoui, B. Abbou, L. Kadiri, I. Lebkiri. (2019). Adsorption of the anionic dye methyl orange on used artificial zeolites: kinetic study and modeling of experimental data. Mediterranean Journal of Chemistry. 9: 311-316.

[32] J. Bensalah, A. El Amri, A. Ouass, O. Hammani, L. Kadiri, H. Ouaddari, S. El Mustapha, A. Zarrouk, B. Srhir. (2022). Investigation of the cationic resin Am® IRC-50 as a potential adsorbent of Co (II): Equilibrium isotherms and thermodynamic studies. Chemical Data Collections. 39: 100879.

[33] J. Bensalah, A. Habsaoui, A. Lebkiri, O. El Khattabi, E. H. Rifi. (2022). Investigation of the cationic resin Amberlite®IRC-50 as a potential adsorbent to remove the anionic dye methyl orange. Desalination and Water Treatment. 246: 280–290.

[34] J. Bensalah, M. Berradi, A. Habsaoui, M. Allaoui, H. Essebaai, O. El Khattabi, A. Lebkiri, E. H. Rifi. (2021). Kinetic and thermodynamic study of the adsorption of cationic dyes by the cationic artificial resin Amberlite®IRC50. Materials Today Proceedings. 45: 7468-7472.

[35] J. Bensalah, M. Galai, M. Ouakki, A. El Amri, H. Boussfiha, A. Habsaoui, O. EL Khattabi, A. Lebkiri, A. Zarrouk, E. H. Rifi. (2022). A combined experimental and thermodynamics study of mild steel corrosion inhibition in 1.0 M hydrochloric solution by the cationic polymer Amberlite®IRC-50 resin extract. Chemical Data Collections. 43: 100976.

[36] M. Allaoui, M. Berradi, H. Taouil, H. Es-Sahbany, L. Kadiri, A. Ouass, J. Bensalah, S. I. Ahmed. (2019). Adsorption of Heavy Métals (nickel) by the Shell Powder of the Coast of Mehdia-Kenitra (Morocco). Analytical and Bioanalytical Electrochemistry. 11 (11): 1547-1558.